Anomalous Kondo Effect in a Quantum Dot at Nonzero Bias

F. Simmel,[1] R. H. Blick,[1] J. P. Kotthaus,[1] W. Wegscheider,[2,*] and M. Bichler[2]
[1]*Center for NanoScience and Sektion Physik, Ludwig-Maximilians-Universität, Geschwister-Scholl-Platz 1, 80539 München, Germany*
[2]*Walter-Schottky-Institut der Technischen Universität München, Am Coulombwall, 85748 München, Germany*
(Received 1 December 1998)

We present measurements on the Kondo effect in a small quantum dot connected strongly to one lead and weakly to the other. The conductance of the dot reveals an offset of the Kondo resonance at zero magnetic field. While the resonance persists in the negative bias regime, it is suppressed in the opposite direction. This demonstrates the pinning of the Kondo resonance to the Fermi levels of the leads.

PACS numbers: 72.15.Qm, 73.23.Hk

The Kondo effect is a well-known phenomenon in solid state physics [1]—the hybridization of conduction electrons with the localized electron spin of a magnetic impurity atom in a metal leads to an enhancement of resistivity at low temperatures. The current interest stems from the fact that mesoscopic devices such as quantum dots allow one to study such complex solid state phenomena on highly controllable systems [2]. The Kondo effect in quantum dots was proposed in early theoretical work [3,4] and then demonstrated in beautiful experiments by Goldhaber-Gordon *et al.* [5,6] and Cronenwett *et al.* [7]. The main features of the Kondo effect in quantum dots are a zero-bias conductance resonance, its specific temperature dependence, and a splitting in a magnetic field.

The novel feature of realizing Kondo physics in a semiconductor quantum dot is the possibility to apply a finite bias V_{sd} across the sample, which is not possible in the case of an ordinary metal. In contrast to previous work we focus on the nonequilibrium properties of a quantum dot in the Kondo regime with the tunneling barriers connected to the leads with different strengths.

The Kondo effect leads to an enhanced local density of states of the quantum dot at the Fermi levels of the electron reservoirs. In the case of symmetric barriers this results in an enhanced conductance at zero bias which is rapidly decreasing for $V_{sd} \neq 0$. Previous measurements [5,7] have been carried out with symmetric barriers, i.e., they met the condition $\Gamma_L = \Gamma_R$, where $\Gamma_{L,R}$ denote the tunnel couplings of the dot to the left and right barrier, respectively. However, the very essence of the Kondo resonance lies in the fact that it is pinned to the Fermi level of each contact which might also lead to the occurrence of a conductance anomaly at nonzero bias. In related work on single charge traps in tunnel junctions a bias splitting was found [8], while it was not perfectly clear how the barrier transmission of the electron trap was involved.

Here, we demonstrate that by tuning a quantum dot into strongly asymmetric coupling an offset of the Kondo conductance resonance to nonzero bias can be observed at $B = 0$ T. This effect is due to the pinning of the resonance to the Fermi level of the more strongly coupled lead.

Following the idea of Kondo physics in a dot we build a small quantum dot similar to the one fabricated by Goldhaber-Gordon *et al.* [5]. Metallic gates are deposited on the top of an AlGaAs/GaAs heterostructure with its two-dimensional electron gas (2DEG) 50 nm below the surface. The 2DEG has a low temperature mobility of 8×10^5 cm^2/V s and a density of 1.6×10^{11} cm^{-2}. A small electron island is formed within the 2DEG by applying negative voltages V_g to the gates [cf. lower inset of Fig. 1(a)]. The measurements are performed in a dilution refrigerator at 25 mK with standard lock-in techniques.

As is shown in Fig. 1(a) we first concentrated on the conventional Coulomb blockade (CB) with symmetric barriers. The level diagram for this situation is sketched in the upper inset: At nonzero bias, electrons can tunnel through the ground state ϵ_0 or excited states of the dot if these are attainable in the energy window opened between the chemical potentials $\mu_{L,R}$ of the leads. The CB diamond displayed in the left of Fig. 2 allows the determination of the total capacitance of the dot [9]. Comparing to the capacitance of a metallic disc, we obtain $r \approx 70$ nm as the radius of the island corresponding to an electron number of 20 and a charging energy of $U = 2.7$ meV. The spin-degenerate mean level spacing can be estimated to be $\Delta = \frac{2\hbar^2}{m^* r^2} \approx 500$ μeV [2]. From the temperature dependence of the line shape the total intrinsic width of the resonances is found to be $\Gamma = \Gamma_L + \Gamma_R = 100$ μeV. We determine the electron temperature to be $T_e \approx 100$–120 mK since the linewidth saturates at this temperature.

In order to tune into the asymmetric Kondo regime we adjusted the transparencies of the barriers by a plunger gate close to the right tunneling contact [gate #2 in the inset of Fig. 1(a)]. As required for the Kondo effect the tunneling barriers are opened first by reducing the applied voltage to the gates #1. Asymmetry is then achieved by adjusting the right barrier opacity with the additional gate #2. Having prepared the dot in such a way, we obtain the peak structure shown in Fig. 1(b). The peaks at $V_{sd} = |\mu_L - \mu_R| = 0$ form pairs for each state with an

 0031-9007/99/83(4)/804(4)$15.00

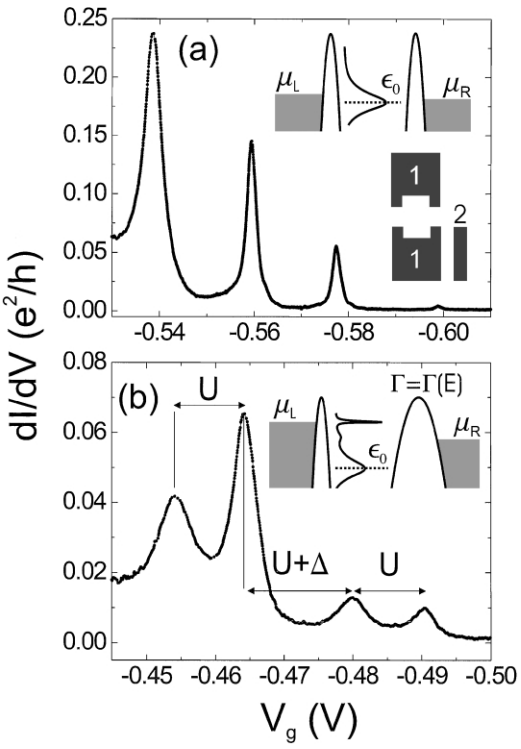

FIG. 1. (a) Quantum dot conductance resonances in the Coulomb blockade regime. The conductance is displayed as a function of the gate voltage V_g applied to gates No. 1 (cf. lower inset). The upper inset schematically shows the effective density of states (DOS) of the quantum dot at almost zero bias. The lower inset shows a schematic of the device. With gates No. 1 the quantum dot is defined, whereas gate No. 2 is used to change the transparency of the right tunneling barrier. (b) Conductance resonances in the case of strong coupling to one lead: due to the spin degeneracy the resonances group into pairs. In the valleys between peaks, separated by the charging energy U, the quantum dot is occupied by an odd number of electrons. In the inset of (b) the effective DOS of the quantum dot with an odd number of electrons is sketched in a nonequilibrium Kondo situation with asymmetric barriers. The Kondo resonance is pinned on the thin barrier side.

odd number of electrons and the conductance background in the valley between the peaks is increased. This peak structure is due to the spin degeneracy of the energy levels of the quantum dot. The energy required for tunneling onto the quantum dot with an odd number of electrons is determined by the charging energy U. In contrast, an electron tunneling onto the dot with an even electron number additionally has to pay the level spacing Δ as it has to occupy a different spatial quantum state. This uniquely identifies the regions of odd electron number in which Kondo phenomena are expected to be observable.

In our case, the barriers define different tunneling rates for the right and left lead. The inset of Fig. 1(b) depicts this relation: Under strong coupling conditions in addition to the ground state ϵ_0 a Kondo resonance appears in the density of states (DOS) of the quantum dot. At nonzero bias this Kondo resonance is split into two resonances each of which is pinned to the chemical potential of the respective lead. Because of the different couplings of the quantum dot to the leads, one of the resonances is enhanced whereas the other is suppressed. To obtain this enhancement, additionally a strong energy dependence of the barrier transparencies has to be assumed, i.e., $\Gamma = \Gamma(E)$. The asymmetry and energy dependence of the tunneling strengths finally result in an enhanced conductance in the CB region at nonzero bias. This is also supported by first numerical simulations [10].

The width of the conductance resonances as determined from their temperature dependence now is $\Gamma \approx 200\ \mu$eV—at the same time the peak height is reduced. As the peak height $\propto \Gamma_L\Gamma_R/(\Gamma_L + \Gamma_R)$ is dominated by the more opaque barrier, this clearly indicates that the tunnel barriers are now tuned into an asymmetric situation. This is verified by estimations of $\Gamma_{L,R}$ from nonlinear transport measurements: The tunnel couplings to the leads can be obtained via $\Delta I \approx e/h\Gamma_{L,R}$, where ΔI is the increase in current when an additional transport channel is opened in resonance with the source or drain contact, respectively [9]. This yields $\Gamma_L \approx 170\ \mu$eV and $\Gamma_R \approx 80\ \mu$eV which is consistent with the temperature dependent measurements: The asymmetry of the tunnel barriers is therefore $\Gamma_L/\Gamma_R \approx 2:1$ and the charging energy changes to $U \approx 1.5$ meV due to the previous retuning of the gates. Accordingly, the Kondo temperature $kT_K \approx (U\Gamma)^{1/2}\exp(-\pi|\mu_{L,R} - \mu_{\mathrm{dot}}|/2\Gamma)$ [4] varies from a minimum value of 20 mK in the valley to 6 K close to the conductance peaks [11]. kT_K is equal to the width of the Kondo resonance. Comparing these values to T_e we find $\Gamma/kT_e \approx 20$ and $T_K/T_e \approx 0.2$–50. From this we can deduce—with regard to the calculations in Ref. [4]—that we are well in the Kondo regime.

The comparison between the conventional CB and the Kondo regime in nonequilibrium is given in the gray-scale plot of the conductance in Fig. 2: In (a) the well-known CB diamond structure is clearly seen. The excited states emerge in the single electron tunneling regions, also revealing lines of negative differential conductance (NDC) [9]. It is commonly assumed that these lines are caused by spin blockade [12] being a consequence of the spin selection rules for transport spectroscopy in a quantum dot. In (b) the coupling of the dot to the leads is strongly enhanced and asymmetric, resulting in a strong deviation from the diamond structure and the appearance of a conductance resonance at small negative bias. This resonance is well pronounced for the upper pair of peaks, while it is only weak for the pair of peaks in the lower part of the plot.

In Fig. 3(a) a close-up of the gray-scale plot of Fig. 2(b) at the position of the resonance around $V_g = -460$ mV is shown: In the CB region around zero bias and between the conductance peaks first-order tunneling processes are forbidden. However, due to the Kondo resonance at the Fermi level of the left barrier the conductance is enhanced

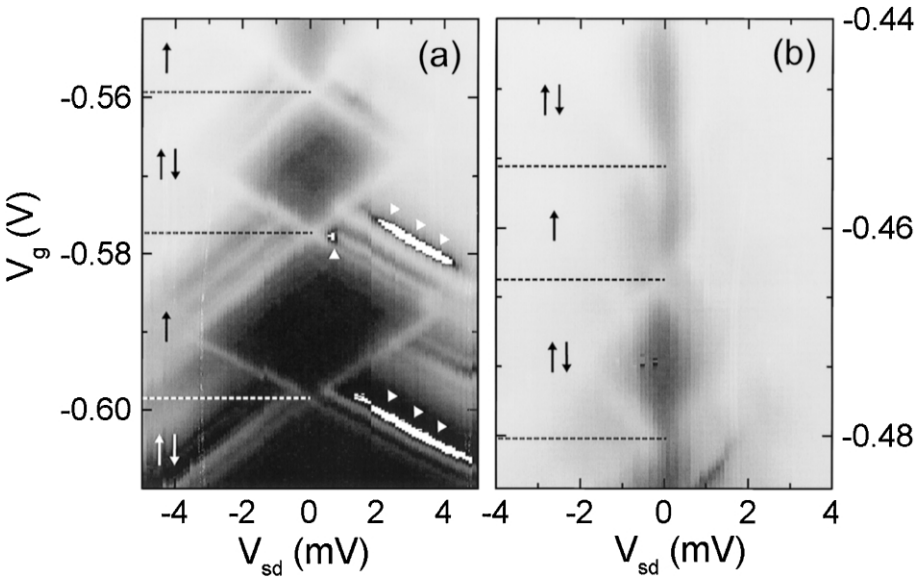

FIG. 2. Gray-scale plot of the bias and gate voltage dependence of the conductance (log scale) (a) in the conventional CB and (b) in the Kondo regime (black: $0 \leq dI/dV \leq 0.05$ μS, white: $dI/dV \geq 20$ μS or $dI/dV < 0$ μS). In (a) the diamond structure and some excited states are well pronounced. The white arrows indicate regions of negative differential conductance related to spin blockade. The arrows on the left give the spin orientation, as derived from the measurements of the Kondo resonance. In (b) the pair structure of the peaks and the Kondo resonance in the valley can clearly be seen. The diamond shape is strongly distorted in this case. The spin orientation is also given (see details in the text).

on the negative bias side. The diamond shape is strongly distorted in the region where the quantum dot is occupied with an odd number of electrons, whereas no effect is visible in the regions above and below where the dot contains an even number of electrons. In the latter regions spin flip processes are inhibited and therefore no Kondo resonance emerges at the Fermi level. Applying a magnetic field perpendicular to the plane of the sample of $B = 0.5$ T only, the Kondo effect is quenched and the regular diamond pattern of CB reappears. A slight increase in magnetic field reduces the tunnel couplings such that the system is tuned out of the Kondo regime.

In Fig. 3(b) the evolution of the Kondo resonance with gate voltage is shown. From the slope $C_{\text{res}}/C_{\text{gate}} \approx 3.6$

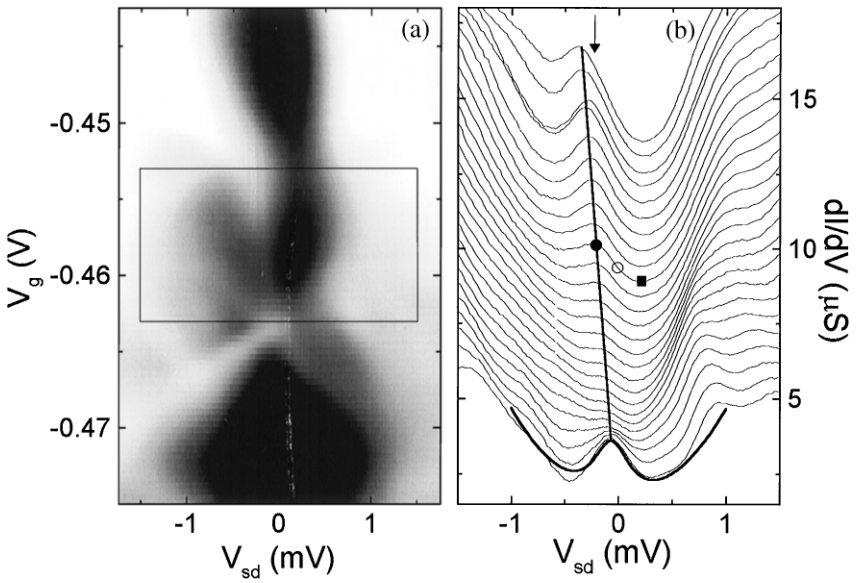

FIG. 3. (a) Magnification of the Kondo resonance for the upper pair of peaks in Fig. 2(b) in a gray-scale plot (linear scale: black, 0 μS; white, 8 μS). The resonance is offset to the negative bias region. (b) The boxed region of (a) displayed with line plots. The lowest trace is taken at $V_g = -0.4634$ V, the uppermost at $V_g = -0.4534$ V. For clarity, the traces are offset by 0.6 μS each. The resonance close to zero bias shifts linearly with the gate voltage. A fit to the resonance in the lowest trace yields a Kondo temperature of 4.9 K.

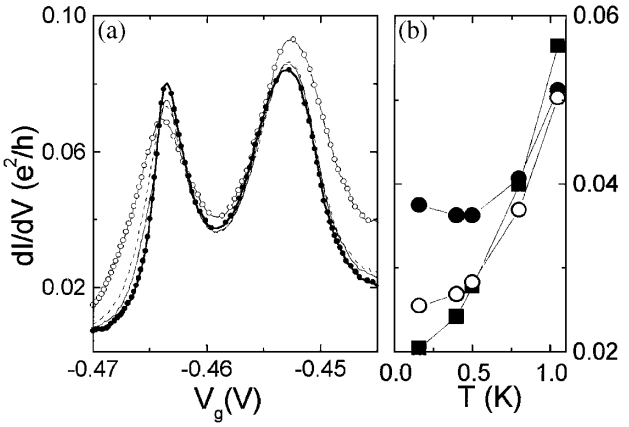

FIG. 4. (a) Temperature dependence of the conductance trace taken at $V_{sd} = -0.19$ mV [indicated by the arrow in Fig. 3(b): (−•−) 160 mK; (———) 400 mK; (– – –) 500 mK; (−∘−) 800 mK]. (b) Temperature dependence of the minimum conductance in the valley between the peaks for negative, zero, and positive bias taken at the points marked in Fig. 3(b).

of the linear shift of the resonance with gate voltage the capacitive coupling to the left reservoir can be estimated to be 60 aF [$C_{\mathrm{res}}/C_{\mathrm{gate}}$ is defined as $-(\delta V_g/\delta V_{sd})_{\mathrm{res}}$ and C_{gate} is related to the peak spacing ΔV_{gate} via $C_{\mathrm{gate}} = e/\Delta V_{\mathrm{gate}}$]. With an on-peak resistance of ≈450 kΩ this yields an RC time of 27 ps corresponding to a decay width of 150 μeV which is fully consistent with our estimation of the coupling to the left reservoir. In the lowest trace a parabola superposed by a Lorentzian has been used to fit the width of the resonance. We obtain 0.42 meV, or $T_K = 4.9$ K, which is in agreement with our earlier estimation of T_K.

Figure 4(a) shows the temperature dependence of a conductance trace taken at negative bias as marked in Fig. 3(b). As expected in the Kondo regime, with lower temperatures the peak positions slightly shift towards each other [7]. At the same time, the conductance in the valley between the peaks passes through a minimum to increase again at the lowest temperature. The temperature dependence of the valley conductance at the positions noted in Fig. 3(b) is shown in Fig. 4(a): Whereas at negative bias Kondo-like behavior is found, at zero bias an intermediate and at positive bias a conventional temperature dependence of the valley conductance is observed.

Consequently, we obtain information on the spin orientation of the ground state in the CB regime as it is marked in Fig. 2(a). The positions of the NDC regions are located at bias voltages larger than found usually. According to Ref. [12] this indicates that the quantum dot has a rather one-dimensional character. For such systems it is guaranteed that the ground state has either zero total spin or spin $S = 1/2$ [12,13]. The spin positions can be related to the positions in the Kondo regime as shown in Fig. 2(b). From this, we further conclude that the Kondo effect is mediated by $S = 1/2$ states and not by higher spin states, as it might generally be possible.

In conclusion, we demonstrated the occurrence of the Kondo effect in a few-electron quantum dot in the case of asymmetric barriers. We observe a pinning of the Kondo resonance to the chemical potential of the left lead. This results in an offset of the conductance anomaly in the CB region to nonzero bias. The position of the anomaly shifts capacitively coupled to one of the reservoirs. The temperature dependence of the valley conductance changes with the applied bias from Kondo-like to conventional behavior. Finally, we were able to show that the Kondo ground state is given by a spin $S = 1/2$ state, instead of a more complex multiplet structure.

We would like to thank D. Goldhaber-Gordon, D. Abusch-Magder, Ch. Bruder, W. Häusler, H. Schoeller, J. König, J. von Delft, D. A. Wharam, J. Weiss, and D. Pfannkuche for helpful discussions and R. J. Warburton for critical reading of the manuscript. This work was funded in part by the Deutsche Forschungsgemeinschaft within Project No. SFB 348.

*Present address: Universität Regensburg, Universitätsstrasse 31, D-93040 Regensburg, Germany.

[1] J. Kondo, Prog. Theor. Phys. **32**, 37 (1964); P. Fulde *et al.,* Solid State Phys. **41**, 1 (1988).
[2] L. P. Kouwenhoven *et al.,* in *Mesoscopic Electron Transport,* edited by H. Grabert, J. M. Martinis, and G. Schön, NATO ASI, Ser. E (Kluwer, Dordrecht, 1997), and references therein.
[3] T. K. Ng and P. A. Lee, Phys. Rev. Lett. **61**, 1768 (1988); L. I. Glazman and M. E. Raikh, Pis'ma Zh. Eksp. Teor. Fiz. **47**, 378 (1988) [JETP Lett. **47**, 452 (1988)].
[4] Y. Meir *et al.,* Phys. Rev. Lett. **70**, 2601 (1993); N. S. Wingreen and Y. Meir, Phys. Rev. B **49**, 11 040 (1994); J. König *et al.,* Phys. Rev. Lett. **76**, 1715 (1996).
[5] D. Goldhaber-Gordon *et al.,* Nature (London) **391**, 156 (1998).
[6] D. Goldhaber-Gordon *et al.,* Phys. Rev. Lett. **81**, 5225 (1998).
[7] S. M. Cronenwett *et al.,* Science **281**, 540 (1998).
[8] D. C. Ralph and R. A. Buhrman, Phys. Rev. Lett. **69**, 2118 (1992); **72**, 3401 (1994).
[9] J. Weis *et al.,* Phys. Rev. Lett. **71**, 4019 (1993).
[10] H. Schoeller, J. König (private communication).
[11] The chemical potential of the quantum dot is defined as $\mu_{\mathrm{dot}} = E(N+1) - E(N)$, where $E(N)$ is the ground state of the N-electron quantum dot.
[12] D. Weinmann *et al.,* Phys. Rev. Lett. **74**, 984 (1995).
[13] W. Häusler (private communication).